Broadband microwave frequency doubler based on left-handed nonlinear transmission lines*

Jie Huang(黄杰)[1,†], Wenwen Gu(顾雯雯)[1], and Qian Zhao(赵倩)[2]

[1] College of Engineering and Technology, Southwest University, Chongqing 400715, China
[2] School of Physical Science and Technology, Southwest University, Chongqing 400715, China

(Received 25 August 2016; revised manuscript received 21 December 2016; published online 13 February 2017)

A bandwidth microwave second harmonic generator is successfully designed using composite right/left-handed nonlinear transmission lines (CRLH NLTLs) in a GaAs monolithic microwave integrated circuit (MMIC) technology. The structure parameters of CRLH NLTLs, e.g. host transmission line, rectangular spiral inductor, and nonlinear capacitor, have a great impact on the second harmonic performance enhancement in terms of second harmonic frequency, output power, and conversion efficiency. It has been experimentally demonstrated that the second harmonic frequency is determined by the anomalous dispersion of CRLH NLTLs and can be significantly improved by effectively adjusting these structure parameters. A good agreement between the measured and simulated second harmonic performances of Ka-band CRLH NLTLs frequency multipliers is successfully achieved, which further validates the design approach of frequency multipliers on CRLH NLTLs and indicates the potentials of CRLH NLTLs in terms of the generation of microwave and millimeter-wave signal source.

Keywords: GaAs planar Schottky diode, frequency multiplier, composite right/left-handed transmission line, monolithic microwave integrated circuit

PACS: 73.61.Ey, 85.40.–e, 84.40.Az, 84.40.Dc **DOI:** 10.1088/1674-1056/26/3/037306

1. Introduction

In the past two decades, an implementation of composite right/left-handed transmission line (CRLH TL) exhibiting anomalous dispersion was proposed to describe the left-handed material (LHM) characterized by antiparallel group and phase velocity, leading to the rapid development of novel microwave devices and circuits.[1–3] Recently, nonlinearity is combined with the anomalous dispersion exhibited by CRLH TLs to form nonlinear left-handed material used to analyze the unique nonlinear wave propagation phenomena,[4–12] among which harmonic generation is very promising and can be used to provide reliable millimeter-wave power for local oscillators due to the lack of an efficient and stable source at millimeter-wave frequency.[13] The performances of composite right/left-handed nonlinear transmission lines (CRLH NLTLs), such as nonlinearity and bandpass response, can be used to effectively generate harmonics in the radio frequency and millimeter frequency.[4] The CRLH NLTLs have been proved to be a typical planar transmission line implementation of metamaterial,[3,14] compatible with the standard GaAs monolithic microwave integrated circuit (MMIC) technology, Si technology, and printed circuit board designs,[15] which show low-loss and broad-bandwidth performances and widely obtain microwave applications.[4–18] Some attempts have been made to design the MMIC harmonic generator.[16,17] When compared with a frequency multiplier based on an FET,[19,20] one based on CRLH NLTLs is self-matched over a much wider frequency range and no additional matching network and filter are needed. The harmonic components are generated and propagate along the CRLH NLTLs, and then the corresponding harmonic signal will be selected and suppressed, which is determined by the anomalous dispersion performances of CRLH NLTLs and the nonlinearity characterized by the nonlinear capacitor.

In this paper, we report the design, fabrication, and measurement of a Ka-band broadband MMIC harmonic generators based on CRLH NLTLs, reveal the means to improve the second harmonic frequency of CRLH NLTLs, and explore the intrinsic relationship between harmonic characteristics and structure parameters of CRLH NLTLs. We thus experimentally investigate the CRLH NLTLs from the viewpoint of the development of harmonic generation.

2. Theoretical analysis and design of the harmonic generator on CRLH NLTLs

CRLH NLTLs periodically consist of a left-handed (LH) series nonlinear capacitance ($C_{\rm L}$), an LH shunt inductance ($L_{\rm L}$), a right-handed (RH) series inductance ($L_{\rm R}$), and a RH shunt capacitance ($C_{\rm R}$), as shown in Fig. 1(a) where $L_{\rm R}$ and $C_{\rm R}$ are the equivalent distributed capacitance and inductance of practical host transmission line (TL) loaded by lumped components of $L_{\rm L}$ and $L_{\rm R}$ shown in Fig. 1(b).[3,21]

*Project supported by the Young Scientists Fund of the National Natural Science Foundation of China (Grant No. 61401373) and the Research Fund for the Doctoral Program of Southwest University, China (Grant No. SWU111030).

†Corresponding author. E-mail: jiehuang@swu.edu.cn

© 2017 Chinese Physical Society and IOP Publishing Ltd

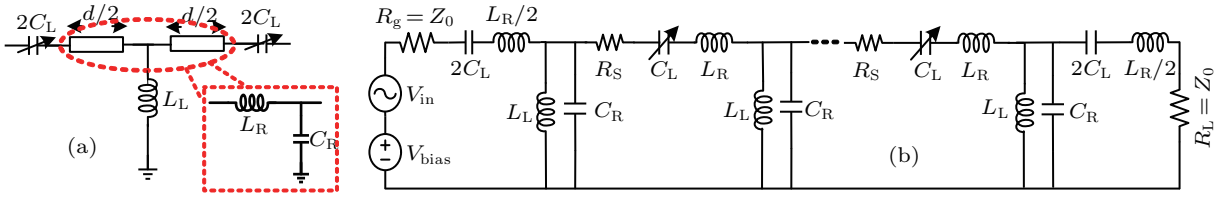


Fig. 1. (color online) (a) CRLH NLTL unit and (b) equivalent circuit model of 5-unit CRLH NLTLs.

CRLH NLTLs represent an anomalous dispersion accurately characterized by[3]

$$\cos(\beta d) = \cos(\beta_{\mathrm{TL}} d)\left(1 - \frac{1}{4\omega^2 L_0 C_0}\right) + \sin(\beta_{\mathrm{TL}} d)\left(\frac{1}{2\omega C_0 Z_0} + \frac{Z_0}{2\omega L_0}\right) - \frac{1}{4\omega^2 L_0 C_0}, \quad (1)$$

and have three characteristic cutoff frequencies: $f_1 = \frac{1}{4\pi\sqrt{L_{\mathrm{L}} C_{\mathrm{L}}}}$, $f_2 = \frac{1}{2\pi\sqrt{L_{\mathrm{R}} C_{\mathrm{L}}}}$, and $f_3 = \frac{1}{2\pi\sqrt{L_{\mathrm{L}} C_{\mathrm{R}}}}$. The propagation characteristics of CRLH NLTLs exhibit adjustable passbands (the lower f_1–f_2 left-handed passband and the upper above f_3 right-handed passband) and f_2–f_3 stopband. The stopband can be closed by the impedance match condition

$$Z_{\mathrm{LH}} = \sqrt{\frac{L_{\mathrm{L}}}{C_{\mathrm{L}}}} = \sqrt{\frac{L_{\mathrm{R}}}{C_{\mathrm{R}}}} = Z_{\mathrm{RH}} = Z_0.$$

When a large signal is implied to the CRLH NLTLs shown in Fig. 1(b), the signal propagates through the nonlinear medium and is distorted according to the nonlinearity of the nonlinear capacitor, and then the second harmonic generation is induced by a balance between the strong nonlinearity and anomalous dispersion effects. The corresponding in-depth theoretical analysis has been made by Kozyrev.[4] The amplitude of the second harmonic in the nth section of a CRLH NLTL $V_2(n)$ is

$$|V_2(n)| = \frac{4K_N V_1^2(0)\sin^2\left(\frac{\beta_1}{2}\right)\sin^2(\beta_1)}{\sin\left(\frac{\beta_2}{2}\right)\left[\sin^2\left(\frac{\beta_2}{2}\right) - \sin^2(\beta_1)\right]} \times \mathrm{e}^{-\alpha n}\left|\sin\left[(\beta_2 - 2\beta_1)n/2\right]\right|, \quad (2)$$

which can be obtained in accordance with the theoretical analysis derived by Kozyrev.[5] It can be seen that the amplitude of the second harmonic largely depends on the phase match between the fundamental wave β_1 and second harmonic wave β_2, and that the frequency of the second harmonic is mainly determined by the anomalous dispersion of CRLH NLTLs characterized by Eq. (1).

The design steps of the harmonic generator on CRLH NLTLs are as follows.

i) Design the nonlinear capacitor with strong nonlinearity and small capacitance, whose fabrication process is compatible with the GaAs MMIC technology. The corresponding epitaxial layers of the nonlinear capacitor are first developed, and then the device model, used to design the harmonic generator on CRLH NLTLs, should be accurately proposed. The capacitance value (C_{L}) needed is determined by the device structure parameters, such as active area and the horizontal space between two electropoles.

ii) Design the LH shunt inductor. The inductance (L_{L}) is designed by the full-wave high frequency structure simulator (HFSS) and the corresponding S-parameter simulated is exported to Agilent's advanced design system (ADS) for harmonic balance (HB) simulation.

iii) Extract the structural parameters of a CRLH NLTL unit without nonlinear capacitors and the number of CRLH NLTL sections (N) by HB simulation in ADS. These parameters correspond to the maximum second harmonic output power at the desired input frequency. Then the equivalent distributed capacitance (C_{R}) and inductance (L_{R}) of host TL of a CRLH NLTL unit can be achieved according to the method in Ref. [21].

iv) Dispersion characteristics analysis, which is carried out to ensure that the desired second harmonic frequency is in the lower LH passband characterized by characteristic frequencies f_1 and f_2, or upper RH passband characterized by characteristic frequency f_3, and that no severe attenuation in the stopband of CRLH NLTLs occurs. The characteristic frequencies (f_1, f_2, and f_3) of CRLH NLTLs can be obtained from the above three steps, and the effective frequency range of the second harmonic can also be determined.

If the desired second harmonic frequency is not in the passband of CRLH NLTLs, steps i–iv will be repeated until the requirement is satisfied by adjusting the active area of the nonlinear capacitor or the geometry structure of the LH shunt inductor.

3. Experiment and measurement

As a demonstration of utilizing the nonlinear transmission line metamaterial as a second harmonic generator, a Ka-band MMIC doubler on CRLH NLTLs has been designed, fabricated, and measured in house. The fabrication process of CRLH NLTLs is similar to those reported in Refs. [17] and [22], and the corresponding photograph of a fabricated five-unit cell CRLH NLTLs with a compact length of 7.16 mm is depicted in Fig. 2(a). Figure 2(b) represents the schematic of a CRLH NLTL unit without planar Schottky varactor diodes

(PSVDs) successfully developed by us shown in Fig. 2(c). Figure 2(d) shows the dc block metal-insulator-metal (MIM) capacitance.

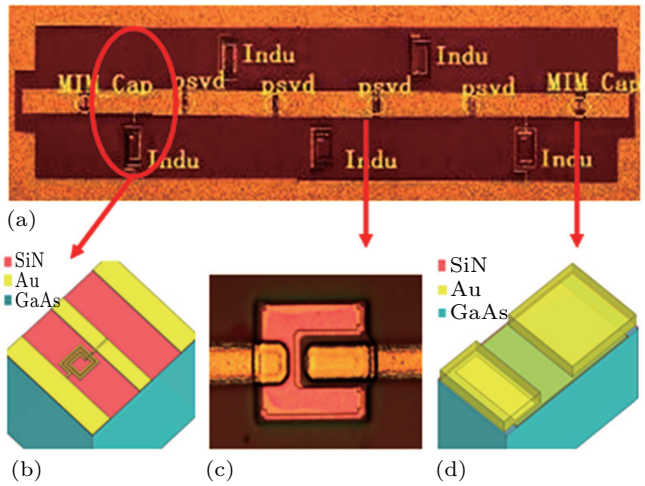


Fig. 2. (color online) (a) Photograph of the 7.16 mm Ka MMIC harmonic generator on CRLH NLTLs, (b) unit cell dimension of CRLH NLTL without PSVDs, (c) photograph of PSVD, and (d) schematic of MIM capacitor.

The passive components of CRLH NLTLs are made in GaAs MMIC technology on the 350 μm GaAs substrate, and specifically the capacitance and inductance are implemented in the form of two metal layers shown in Figs. 2(b) and 2(d). All TLs are in the coplanar waveguide (CPW) configuration and the sophisticated via-hole processes are avoided. The spiral inductor, with 10 μm strip width (L_W), 10 μm gap (L_S), inner radium of 40 μm (L_R), and turn number of 2.5 (L_N), has an inductance of 1.6 nH at 5 GHz. The CPW, with 100 μm center signal linewidth (W), 260 μm gap (G) between the center signal line and the two side coplanar ground plane, and 740 μm host CPW length (D) of a CRLH NLTL unit, has characteristic impedance (Z_0) of 75 Ω. When compared with the simulated S-parameter by HFSS, the measured result by the 8510C network analyzer from 0.1 to 40 GHz is shown in Fig. 3(a), and an excellent agreement is obtained.

The nonlinear capacitances are also implemented by PSVDs shown in Fig. 2(c) in GaAs MMIC technology, and the corresponding GaAs epitaxial layers for PSVD developed by us were grown by MBE. A 1-μm-thick n^+ active layer doped to 5×10^{18} cm^{-3} was first grown on a 350 μm GaAs substrate, followed by a 0.6-μm-thick n layer doped with 5×10^{16} cm^{-3} concentration.[23,24] The corresponding C–V characteristic of PSVD with a Schottky contact area (S) of 160 μm^2 shown in Fig. 3(b) is characterized by $C_j = C_{j0}/\left(1-\frac{V}{V_{bi}}\right)^M$, where C_{j0} is zero-bias junction capacitance of 125 fF, V_{bi} is the barrier potential of 0.65 V, and M is the index factor of 0.35 depending on the diode doping profile. The PSVD has a high breakdown voltage of 22 V and a strong nonlinearity weighed by the capacitance ratio of 5.4 between the maximum capacitance C_{max} and minimum capacitance C_{min} of PSVD over the range of applied voltages from reverse 10 V to forward 0.6 V. The extracted equivalent circuit model of PSVD in Ref. [24] is used to design the Ka-band harmonic generator on CRLH NLTLs.

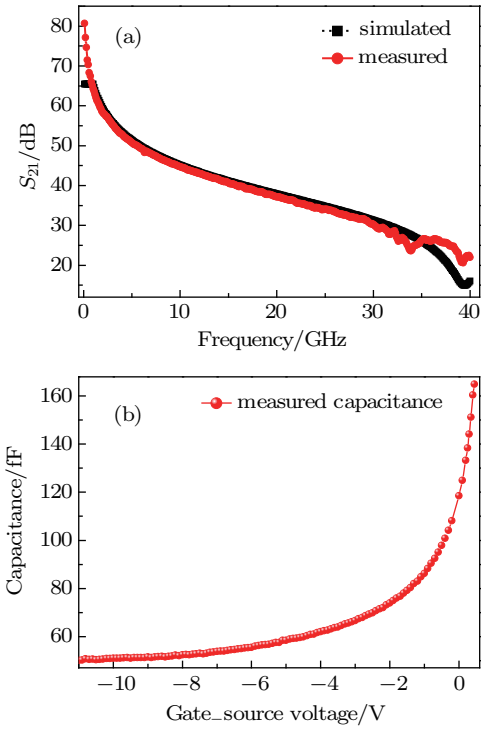


Fig. 3. (color online) (a) The measured and simulated S-parameter characteristic of a CRLH NLTL unit without PSVDs. (b) The measured C–V characteristic of nonlinear capacitance in a CRLH NLTL unit.

When compared with the simulated S-parameters result, based on the fact that passive components are obtained by full-wave HFSS and nonlinear PSVDs are replaced by the equivalent circuit model, the measured S-parameters magnitude of five-unit CRLH NLTLs is represented in Fig. 4, and a good agreement is observed between them. The small deviation between them is caused by the fabrication tolerance. The measured S_{21} exhibits a stopband in the frequency range from 10.5 GHz (f_1) to 18.5 GHz (f_2), which is consistent with the theoretical dispersion one from 11.2 GHz (f_1) to 20.2 GHz (f_2). Experimentally, we define the corresponding frequency as the cutoff frequency when S_{21} is −10 dB. The return loss in the second harmonic frequency is better than 10 dB and the good impedance match ensures that as much input power as possible is transmitted to the output port of five-unit CRLH NLTLs. Nevertheless, there are relatively large deviations between the simulation and the measurement results in the high frequency band. The deviation is mainly due to the repeatability of the fabrication process and the accuracy of the equivalent large signal model of the Schottky diode, because the simulated and measured CRLH NLTL unit without PSVDs is in excellent agreement. It partly comes from the MIM capacitor. First, the fabrication processes of the Schottky diode are developed to achieve Schottky diodes with high performances and

the corresponding equivalent model. Then, the corresponding fabrication process is used to fabricate the doubler based CRLH NLTLs, and the reproducibility of the process results in the deviation. Therefore, a more stable and reliable process is needed.

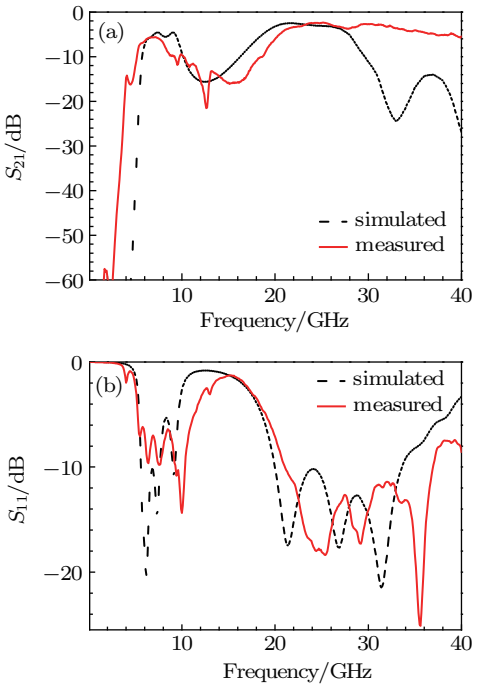


Fig. 4. (color online) Comparison of the measured and simulated *S*-parameters characteristic for the Ka-band MMIC harmonic generator on five-unit CRLH NLTLs.

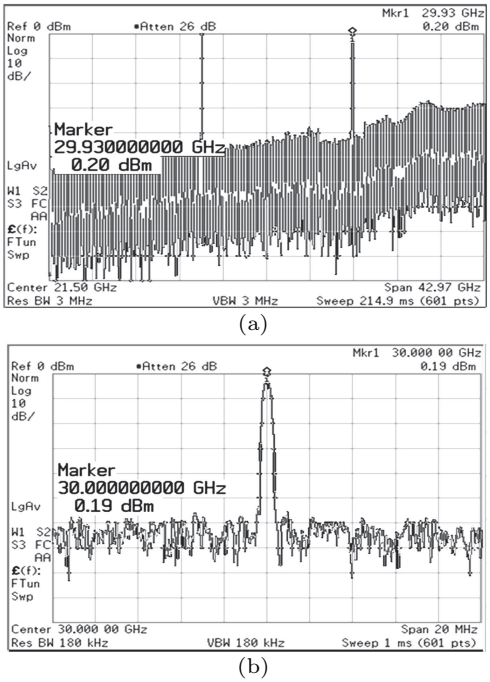


Fig. 5. Spectrum of the harmonics of the Ka-band MMIC harmonic generator on CRLH NLTLs fed by 15 GHz 20 dBm input signal.

The large signal performances of the Ka-band MMIC harmonic generator on CRLH NLTLs were measured on-wafer by an Agilent E3334A (3 Hz to 42.9 GHz) spectrum analyzer and the input signal was provided by an Agilent E8257D vector signal generator. When a 15 GHz 20 dBm input signal was fed into CRLH NLTLs, it can be found from Fig. 5(a) that the 30 GHz second harmonic signal is reliably observed, which represents a relatively high output power of 4.2 dBm including system loss calibration of about 3.95 dBm. The expanding second harmonic shown in Fig. 5(b) shows much lower phase noise of −107 dBc/Hz@100 kHz, which is nearly close to the theoretical value of −116 dBc/Hz@100 kHz when an input signal of −110 dBc/Hz@100 kHz at 10 kHz offset is doubled with 6 dB theoretical phase degradation.

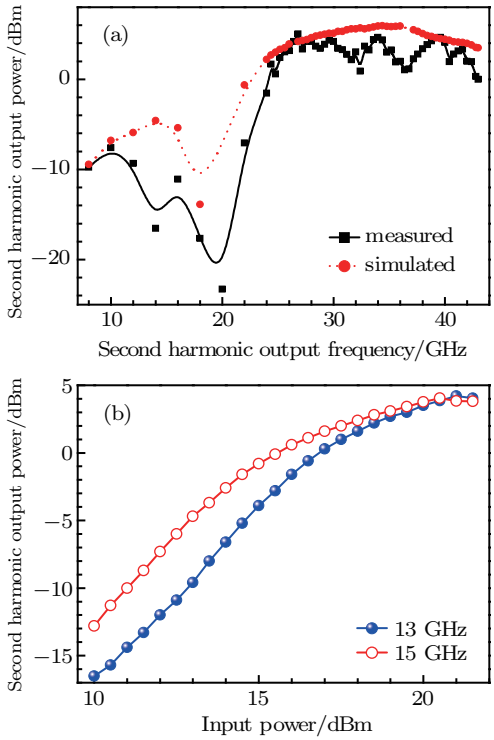


Fig. 6. (color online) (a) Measured and simulated second harmonic output power versus second harmonic frequency of the Ka-band MMIC harmonic generator on CRLH NLTLs fed by 20 dBm input signal at 0 V bias. (b) Measured second harmonic output power versus input power of harmonic generator on CRL NLTLs fed by 13 and 15 GHz input signal.

The fabricated Ka-band MMIC harmonic generator was measured as a function of second harmonic frequency and input power. As shown in Fig. 6(a), the simulated second harmonic output power of CRLH NLTLs is in good agreement with the measured one over the frequency range from 7 GHz to 43 GHz at 0 V bias for PSVDs. The maximum output power $((P_{2\text{out}})_{\max})$, conversion efficiency $((\eta_{2\text{out}})_{\max})$, and the corresponding frequency $((f_{2\text{out}})_{\max})$ of the second harmonic is 7.85 dBm, 6.1%, and 29.6 GHz, respectively. As can be seen from Fig. 6(b), the measured second harmonic output power is linear with the input power and then a notable saturation performance determined by the breakdown voltage and nonlinearity of PSVDs is observed when the input signal of 13 GHz and

15 GHz is fed, respectively. Moreover, the second harmonic output power of 30 GHz is more than that of 26 GHz over the input power range from 10 dBm to 21 dBm, and the output second harmonic is saturated to the same output power of 7.85 dBm at 13 and 15 GHz input frequency. The magnitude of the second harmonic output power is very sensitive to frequency variations because of anomalous dispersion of CRLH NLTLs.

To explore the intrinsic relationship between structure parameters of CRLH NLTLs and harmonic characteristics such as second harmonic bandwidth and frequency range, output power, and conversion efficiency, the K-band MMIC harmonic generator on CRLH NLTLs was also used to compare.[17] Table 1 compares the structure parameters and harmonic characteristics of K-band and Ka-band doublers on CRLH NLTLs. It can be seen that decreasing the number of turns of the shunt inductor leads to the increase of corresponding peak second harmonic frequency, expending the frequency range of the second harmonic with above 0 dBm output power, and at the same time the peak output power and conversion efficiency of the second harmonic reduces. The relationship has been theoretically verified by the anomalous dispersion of CRLH NLTLs that smaller $L_{\rm L}$, $L_{\rm R,}$ and $C_{\rm R}$ determined by the structure parameters lead to the corresponding increase of the three characteristic cutoff frequencies f_1, f_2, and f_3. The frequency of the second harmonic must be in the lower f_1–f_2 left-handed passband and the upper above f_3 right-handed passband so that severe attenuation of the harmonics will not happen. Therefore, the frequency of the second harmonic is significantly improved from K-band to Ka-band due to the structure parameters adjustment of CRLH NLTLs. It is expected that the second harmonic frequency can be further expanded to millimeter-wave and even terahertz frequency by reducing the Schottky active area of PSVD with smaller capacitance $C_{\rm L}$ and stronger nonlinearity.

Table 1. Comparison of K-band and Ka-band MMIC harmonic generator on CRLH NLTLs.

Parameter	Ka-band	K-band[17]	Parameter	Ka-band	K-band[17]
LH Inductor	$L_{\rm W} = L_{\rm S} = 10$ μm	$L_{\rm W} = L_{\rm S} = 10$ μm	Z_0	73 Ω	81 Ω
	$L_{\rm R} = 40$ μm, $L_{\rm N} = 2.5$	$L_{\rm R} = 40$ μm, $L_{\rm N} = 3.5$	N	5	5
LH Inductance	1.6 nH@5 GHz	2.9 nH@5 GHz	f_1	5.1 GHz	3.7 GHz
$C_{\rm MIM}$	0.25 pF	0.25 pF	f_2	10.5 GHz	6.8 GHz
PSVD	$S = 160$ μm^2	$S = 160$ μm^2	f_3	18.5 GHz	17.6 GHz
CPW TL	$D = 740$ μm, $W = 100$ μm, $G = 260$ μm	$D = 920$ μm, $W = 83$ μm, $G = 290$ μm	$(f_{\rm 2out})_{\rm max}$	34 GHz	26.4 GHz
			$(P_{\rm 2out})_{\rm max}$	4.65 dBm	6.7 dBm
$L_{\rm R}$	0.49 nH	0.65 nH	$(\eta_{\rm 2out})_{\rm max}$	2.92%	4.7%
$C_{\rm R}$	0.0983 pF	0.115 pF	$p_{\rm 2out} > 0$	24.4–43 GHz	16.4–35.2 GHz

Several harmonic generators on CRLH NLTLs are summarized in Table 2. It can be seen that those by MMIC technology have significant advantages over those by hybridizing in harmonic performances such as frequency, output power, and conversion efficiency of the second harmonic. Because of the high-frequency capability of the PSVDs and the simplicity of the design and fabrication, the design approach reported here can be readily applied to higher frequencies for a frequency multiplier on CRLH NLTLs. It has been predicted that the third harmonic will be dominant if the nonlinear capacitor of CRLH NLTL structured by two back-to-back varactor diodes with symmetrical C–V characteristic is adopted.[4] Therefore, based on a similar design method, the frequency of effective harmonic is expected to be further improved by means of triples on CRLH NLTLs, which will be performed in future.

Table 2. Comparison of harmonic generator on CRLH NLTLs.

Reference	CRLH NLTL Unit	$p_{\rm 2out} > 0$	$p_{\rm in}$	$(p_{\rm 2out})_{\rm max}$	$(\eta_{\rm 2out})_{\rm max}$	Technology
Ref. [9]	4	4.076 GHz	18 dBm	0 dBm	1.58%	hybrid
Ref. [5]	4	2.87 GHz	17.9 dBm	10.72 dBm	19%	hybrid
K-band[17]	5	16.4–35.2 GHz	20 dBm	7.85 dBm	4.7%	MMIC
Ka-band	5	24.4–56 GHz	20 dBm	7.85 dBm	2.92%	MMIC

4. Conclusion

CRLH NLTLs metamaterial is successfully used to design a broadband Ka-band MMIC harmonic generator. A good agreement between the measured and simulated harmonic performances effectively validates the proposed design procedure of the harmonic generator on CRLH NLTLs. It has been demonstrated that a 7.85-dBm peak second harmonic output power at 29.6 GHz and low phase noise of 107 dBc/Hz@100 kHz at 10-kHz offset are successfully obtained, and that the second harmonic output power is above 0 dBm over every broad frequency range from 24.4 to 43 GHz

when a 20 dBm input large signal is fed. The second harmonic output power is sensitive to frequency and the corresponding harmonic frequency should be in the passband of CRLH NLTLs to avoid severe attenuation in the stopband due to RH and LH TL impedance mismatch. When compared with the Ka-band MMIC harmonic generator, another K-band one based on the same design procedure is also used to explore the intrinsic relationship between harmonic characteristics and structure parameters of CRLH NLTLs such as host TL and rectangular spiral inductor. It has been experimentally demonstrated that the second harmonic frequency is determined by the anomalous dispersion of CRLH NLTLs and can be significantly improved from K-band to Ka-band by effectively reducing the LH shunt inductance and RH equivalent distributed capacitance C_{R} and inductance L_{R} of the host CPW of a CRLH NLTL unit, which indicates the potentials of CRLH NLTLs in terms of the generation of microwave and millimeter-wave signal source. It will be expected that reducing the Schottky active contact area and using back-to-back symmetrical C–V PSVDs in CRLH NLTLs lead to further improvement of the harmonic frequency although more challenges will occur.

References

[1] Veselago V G 1968 *Sov. Phys. Usp.* **10** 509

[2] Caloz C and Itoh T 2003 *IEEE MTT-S International Microwave Symposium Digest*, June 8, 2003, Philadelphia, USA, p. 195

[3] Eleftheriades G V, Iyer A K and Kremer P C 2002 *IEEE Trans. Microw. Theory Tech.* **50** 2702

[4] Kozyrev A B and van der Weide D W 2005 *IEEE Trans. Microw. Theory Tech.* **53** 238

[5] Kozyrev A B, Kim H, Karbassi A and van der Weide D W 2005 *Appl. Phys. Lett.* **87** 121109

[6] Kozyrev A B, Kim H and van der Weide D W 2006 *Appl. Phys. Lett.* **88** 264101

[7] Kozyrev A B and van der Weide D W 2010 *Appl. Phys. Lett.* **96** 104106

[8] Kozyrev A B, Kim H and van der Weide D W 2007 *Appl. Phys. Lett.* **91** 254111

[9] Kim H, Kozyrev A B, Karbassi A and van der Weide D W 2007 *IEEE Trans. Microw. Theory Tech.* **55** 571

[10] Wang Z B, Feng Y J, Zhu B, Zhao J M and Jiang T 2010 *J. Appl. Phys.* **107** 094907

[11] Simion S, Marcelli R, Bartolucci G, Proietti E, Angelis G D and Lucibello A 2010 *35th Infrare Millimeter and Terahertz Waves International Conference*, September 5, 2010, Roma, Italy, p. 1

[12] Simon S, Bartolucci G and Marcelli R 2009 *International Semiconductor Conference*, October 12, 2009, Sinaia, Romania, p. 345

[13] Choudhury D, Frerking M A and Batelaan P D 1993 *IEEE Trans. Microw. Theory Tech.* **41** 595

[14] Li H Y, Zhang Y W, Zhang L W, He L, Li H Q and Chen H 2007 *J. Appl. Phys.* **102** 033711

[15] Zhao Y, Wu L S, She H C, Zhang Y T and Chen T S 2016 *Chin. Phys. B* **25** 067306

[16] Dong J R, Huang J, Tian C, Yang H and Zhang H Y 2011 *J. Semiconductors* **32** 095003

[17] Huang J, Dong J R, Yang H, Zhang H Y, Tian C and Guo T Y 2011 *IEEE Trans. Microw. Theory Tech.* **59** 2486

[18] Tong W, Hu Z R, Chua H S, Curtis P D, Gibson A A P and Missous M 2007 *IEEE Trans. Microw. Theory Tech.* **55** 1794

[19] Seo S, Jeong Y, Lim J, Gray B and Kenney S 2007 *IEEE MTT-S International Microwave Symposium Digest*, June 3, 2007, Honolulu, USA, p. 2185

[20] Jadpum P, Tangit J and Bunnjaweht S 2009 *6th Electric Engineering/Electronics and Information Technology Conference*, May 6, 2009, Pattaya, Thailand, p. 521

[21] Lai A, Itoh T and Caloz C 2004 *IEEE Micow. Mag.* **5** 34

[22] Huang J, Dong J R, Yang H, Zhang H Y, Tian C and Guo T Y 2011 *Chin. Phys. B* **20** 060702

[23] Huang J, Zhao Q, Yang H, Dong J R and Zhang H Y 2013 *Chin. Phys. B* **22** 127307

[24] Huang J, Zhao Q, Yang H, Dong J R and Zhang H Y 2014 *J. Semiconductors* **35** 054006